Organic & Biomolecular Chemistry

PAPER

Mimicking the 2-oxoglutaric acid signalling function using molecular probes: insights from structural and functional investigations†

Cite this: *Org. Biomol. Chem.*, 2014, **12**, 4723

Yang Wang,‡[a,b] Xinjun Liu,‡[a,b] Erik Laurini,[c] Paola Posocco,[c,d] Fabio Ziarelli,[e] Maurizio Fermeglia,[c,d] Fanqi Qu,[b] Sabrina Pricl,[c,d] Cheng-Cai Zhang[f] and Ling Peng*[a]

Received 25th March 2014,
Accepted 9th May 2014

DOI: 10.1039/c4ob00630e

www.rsc.org/obc

2-Oxoglutaric acid (2-OG) has gained considerable attention because of its newly discovered signalling role in addition to its established metabolic functions. With the aim of further exploring the signalling function of 2-OG, here we present a structure–activity relationship study using 2-OG probes bearing different carbon chain lengths and terminal groups. Our results highlight the importance of the five-membered carbon molecular skeleton and of the two carboxylic terminals in maintaining the signalling functions of the parent molecule 2-OG. These findings provide valuable information for designing new, effective molecular probes able to dissect and discriminate the newly discovered, complex signalling role of 2-OG from its canonical activity in metabolism.

Introduction

2-Oxoglutaric acid (2-OG, Scheme 1), one of the key intermediates in the Krebs cycle, constitutes an important precursor in the synthesis of biomolecules and in the production of cellular energy. Beyond its canonical functions in metabolism, 2-OG has recently gained considerable attention as a key signalling molecule in different organisms.[1–5] Indeed, several studies indicate that 2-OG plays critical roles in many signalling pathways such as, among others, regulation of the balance of carbon/nitrogen metabolism,[6–8] epigenetic regulation mediated by 2-OG-dependent oxygenases,[9] and generation of the "onco-metabolite" 2-hydroxyglutarate *via* misregulated metabolism in various cancers.[10] Over the past few years, we have been particularly interested in studying the signalling function of 2-OG in regulating the coordination of carbon/nitrogen metabolism in *Anabaena*, cyanobacteria able to fix the molecular nitrogen in air in the absence of a combined nitrogen source. Since 2-OG can be rapidly metabolized *in vivo*, it is difficult to discriminate its signalling role from its metabolic functions. Thus, we synthesized various non-metabolisable 2-OG mimics (Scheme 1) to specifically investigate the 2-OG signalling role. Previous results obtained with DFPA and 2-MPA, two 2-OG mimics bearing modifications at the carbonyl group at the C2 position, demonstrated for the first time the signalling role of 2-OG in sensing nitrogen starvation in *Anabaena*.[3,11] Further structure–activity relationship analysis using 2-OG mimics harbouring structural variations at the C4 position led us to the discovery that DFMPA and DMPA are

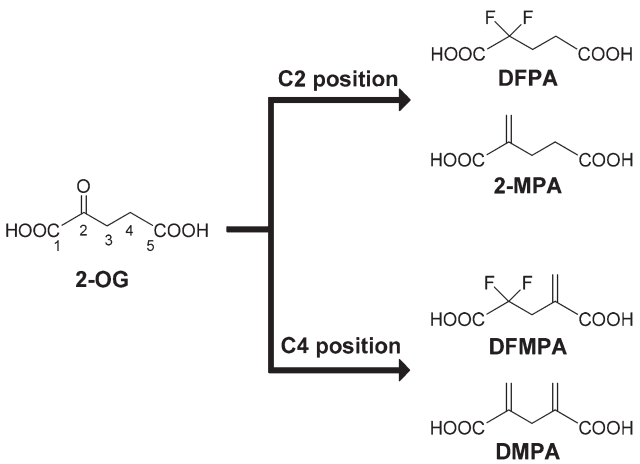

Scheme 1 2-Oxoglutaric acid (2-OG) and its mimics previously developed by us.[3,11–13]

[a]*Aix-Marseille Université, CNRS, CINaM UMR 7325, 13288 Marseille, France. E-mail: ling.peng@univ-amu.fr*
[b]*College of Chemistry and Molecular Sciences, Wuhan University, P. R. China*
[c]*Molecular Simulation Engineering (MOSE) Laboratory, Department of Engineering and Architecture (DEA), University of Trieste, Italy*
[d]*National Interuniversity Consortium for Material Science and Technology, Research Unit MOSE-DEA, University of Trieste, Italy*
[e]*Aix-Marseille Université, Spectropôle, CNRS FR 1739, Marseille, France*
[f]*Laboratoire de Chimie Bactérienne, CNRS UMR 7283, Marseille, France*
† Electronic supplementary information (ESI) available: ^{1}H and ^{13}C NMR spectra of probes **1** and **4**. See DOI: 10.1039/c4ob00630e
‡ These authors contributed equally to this work.

also able to mimic the signalling role of 2-OG in *Anabaena*.[12,13] These surprising yet interesting findings demonstrated that stringent structural alterations at the C2 and C4 positions can be tolerated in 2-OG analogues, endowing these molecules with the regulatory function of 2-OG in *Anabaena via* binding the corresponding receptor.

In order to gain further insight into the structure–activity relationship of 2-OG analogues in mimicking 2-OG biological functions, we questioned whether the two terminal carboxylic functionalities and the length of the molecular carbon skeleton also constituted essential structural requirements for the signalling role of 2-OG. Although these molecular features already characterized some 2-OG probes previously developed for studying the signalling role of 2-OG,[3,11–14] no direct experimental evidence has revealed or proven the significance/prerequisites of these structural elements in the 2-OG signalling function so far. With the goal of providing a clear-cut and straightforward answer to this question, we then designed four new 2-OG probes **1–4** (Scheme 2) bearing chemical variations both at the carboxylic functionalities and the carbon skeleton. All new probes feature a vinyl group at the C2 position which, besides acting as a mimic of the carbonyl functionality in 2-OG, allows easy and convenient chemical synthesis and imparts sufficient chemical and biological stability. Probes **1** and **2** were specifically devised to investigate the significance of the two carboxylic acid terminals in 2-OG. Probe **1** features two tetrazole rings as bioisosteres[15] of the carboxylic acid functionalities in 2-OG. Since the lipophilicity of the planar tetrazole cycle is reported to be higher than that of the carboxylic group,[15] this will likely favour the penetration of probe **1** across the negatively charged cellular membrane under physiological conditions. With the same goal of increasing cell membrane penetration, probe **2** contains two lipophilic methyl ester groups in place of the carboxylic terminals. Notably, probe **2** can be considered as a prodrug of 2-OG; indeed, we expected that probe **2** could be hydrolysed by cellular enzymes to yield 2-OG which, eventually, might exert the corresponding signalling function. Probes **3** and **4** are characterized by a molecular scaffold of 4 and 6 carbon atoms, respectively; these compounds were conceived to explore the importance of the carbon skeleton length in 2-OG analogues.

Here we report the detailed synthesis and biological evaluation of all new probes **1–4**. Our studies revealed that the two carboxylic acid terminals and the 5-membered carbon skeleton in 2-OG are both essential to retain its signalling function, even minor structural alteration or modification not being tolerated for mimicking the signalling role of 2-OG. These findings are important *per se* and instrumental for the design of new, effective and high affinity 2-OG probes that facilitate the process of deciphering the signalling pathway of 2-OG.

Results and discussion

We prepared probe **2** using our previously developed protocol,[11] and purchased **3** from a commercial source. The synthesis of **1** and **4** was successfully achieved using the strategies presented in Scheme 3. Treating 2-methyleneglutaronitrile with NaN_3 *via* Huisgen cycloaddition afforded probe **1**.[16–18] To synthesize **4**, we first obtained the corresponding ethylester precursor by condensing ethyl 4-bromobutyrate, triethyl phosphonoacetate and formaldehyde *via* an Horner–Wadsworth–Emmons (HWE) reaction[20] before alkaline hydrolysis to yield **4**.

With all four probes at hand, we assessed their ability to mimic the signalling function of 2-OG in sensing nitrogen starvation in cyanobacteria *Anabaena*. *Anabaena* represents an excellent biological model to investigate the signalling role of 2-OG in nitrogen metabolism since, in response to combined-nitrogen deprivation,[21,22] they produce morphologically distinct heterocysts which can be easily observed and identified under a microscope. In addition, this heterocyst differentiation can be repressed at early stages if a combined nitrogen source such as ammonium or nitrate is supplied to the growth medium. In previous studies, we clearly showed the 2-OG-mimicking capacity of non-metabolisable 2-OG analogues such as DFPA, 2-MPA, DFMPA and DMPA in inducing heterocyst formation even under repressive conditions (*i.e.*, in the presence of high ammonium concentration).[3,11–13] However, none of the new probes **1–4** could trigger heterocyst formation (data not shown). Moreover, probe **2** seemed to be toxic for *Anabaena* and induced rapid cell death through an as-yet

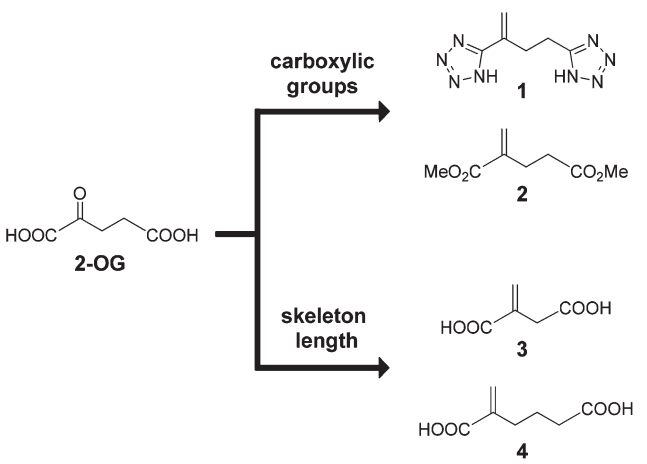

Scheme 2 New 2-OG probes **1–4** studied in this work.

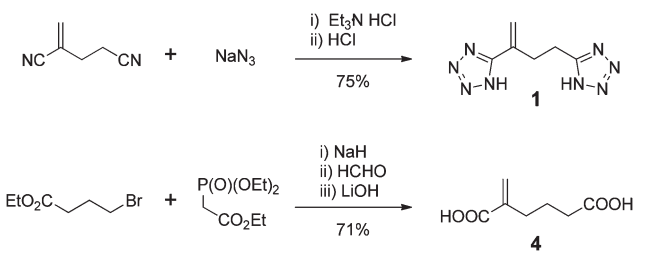

Scheme 3 Synthesis of probes **1** and **4**.

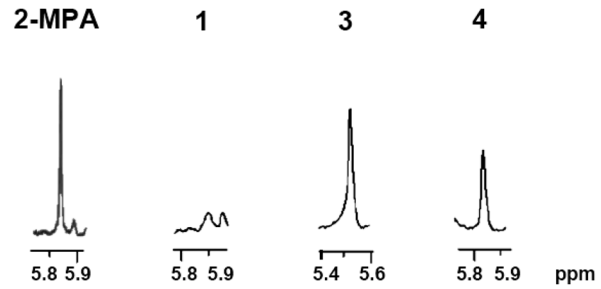

Fig. 1 ^{1}H HRMAS NMR study on the uptake of **1**, **3** and **4** in the KGTP strain compared to the control reference 2-MPA.

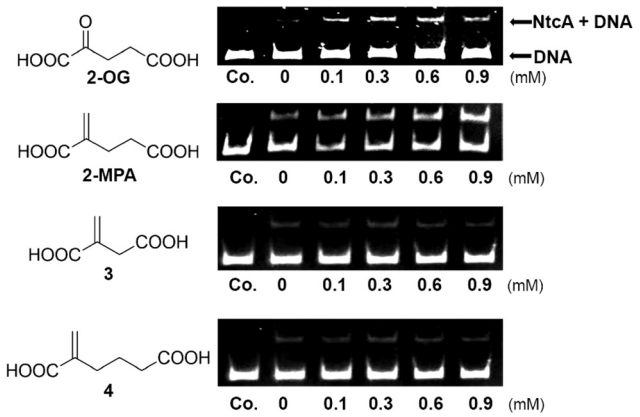

Fig. 2 DNA binding affinity of NtcA at various concentrations of 2-OG, 2-MPA, and probes **3** and **4**. Co: DNA fragment without NtcA.

unclear pathway.[23] Due to our concerns over the toxicity of **2**, this probe was no longer considered in further studies.

In order to understand why **1**, **3** and **4** could not trigger heterocyst differentiation, we next examined their cellular uptake using KGTP, a recombinant strain of *Anabaena* that expresses the 2-OG permease KgtP. This was expected to facilitate the uptake of 2-OG and its probes (all negatively charged under physiological conditions) across the cell membrane.[3,11–13,24,25] To monitor the uptake of these probes by the KGTP strain, we used ^{1}H High Resolution Magic Angle Spinning (HRMAS) NMR, an excellent non-destructive method for *in vivo* analysis of the metabolic profiles of the whole cells.[26] For each probe, we inspected the characteristic ^{1}H NMR signals associated with the vinyl group around 5–6 ppm. As seen in Fig. 1, probe **1** showed poor cellular uptake compared with the positive control 2-MPA, suggesting that this molecule could probably not be recognized by the 2-OG permease. This is somewhat not surprising as the tetrazole heterocycle, though bioisostere of the carboxylic functionality, might considerably shift the molecular conformation of **1** from that of 2-OG. Accordingly, the structural deviation of **1** from 2-OG alongside with its inability to cross the cell membrane could be the main reasons underlying the failure of this molecule in inducing heterocyst formation in *Anabaena*. Conversely, probes **3** and **4** showed notable cellular uptake. This might be ascribed to the effective recognition of **3** and **4** by the 2-OG permease and their subsequent, favoured cell penetration. These results definitely ascertain the major role played by the two 2-OG carboxylic groups in determining its effective cellular uptake.

Although **3** and **4** displayed good uptake in *Anabaena*, once internalized, they could not induce heterocyst formation. In order to formulate a plausible rationale for these findings, we went on to study the effect of **3** and **4** on the DNA binding activity of the 2-OG receptor NtcA, a transcription factor which regulates nitrogen metabolism in *Anabaena*.[3,11–14] NtcA is essential for the initiation of heterocyst differentiation, and 2-OG enhances the DNA binding affinity of NtcA (Fig. 2). As clearly shown in Fig. 2, the binding of NtcA to DNA was enhanced by increasing concentrations of 2-OG and its active mimic 2-MPA. In contrast, neither **3** nor **4** could increase DNA/NtcA binding, suggesting that a low affinity for NtcA could underlie the inability of **3** and **4** to trigger heterocyst differentiation in *Anabaena*.

To further substantiate the NtcA binding failure of probes **3** and **4**, we carried out atomistic molecular dynamics (MD) simulations of the corresponding NtcA/probe complexes.[27–31] In our previous studies,[12,13] we found that, for 2-OG and all successful 2-OG mimics including 2-MPA, two efficient salt bridges between the two charged carboxylic groups of 2-OG and the NtcA side chains of Arg88 and Arg129, respectively, constitute the main stabilizing contribution towards their binding to NtcA. Our current modelling data show that, in the case of the new derivatives **3** and **4**, these stabilizing interactions can occur only if the vinyl moieties in these compounds adopt a reverse orientation with respect to 2-OG within the NtcA binding site (Fig. 3). However, by assuming this different binding pose, the network of four H-bonds anchoring 2-OG (and 2-MPA) to the NtcA residues Phe75,

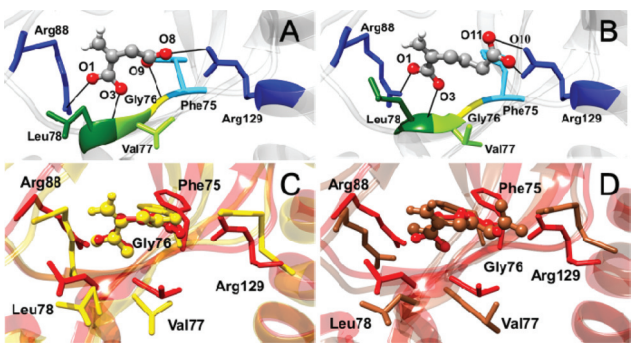

Fig. 3 Equilibrated MD snapshot of **3** and **4** in complex with NtcA. Zoomed view of **3** (A) and **4** (B) within the NtcA binding pocket. Compounds **3** and **4** are shown as atom-coloured balls-and-sticks (O, red; C, grey). The H-atoms of the methylene group(s) are highlighted in white. Black lines denote hydrogen bond and salt bridge interactions. NtcA residues directly involved in binding **3** and **4** are shown as labelled, coloured sticks: Phe75 (light blue), Gly76 (yellow), Val77 (green), Leu78 (dark green), Arg88 and Arg129 (both in blue). (C) Superposition of NtcA/**2-OG** (red) and NtcA/**3** (gold) binding modes. (D) Superposition of NtcA/**2-OG** (red) and NtcA/**4** (sienna) binding modes. In all panels, water molecules, ions, and counterions are omitted for clarity.

Table 1 Enthalpy (ΔH_{bind}), entropy ($-T\Delta S_{bind}$) and total free energy of binding (ΔG_{bind}) for **3** and **4** in complex with NtcA[a]

Compound	**3**	**4**	2-OG	2-MPA
ΔH_{bind}	−44.4 (0.5)	−45.2 (0.5)	−50.7 (0.4)	−48.3 (0.5)
$-T\Delta S_{bind}$	34.9 (0.9)	36.0 (0.7)	35.2 (0.8)	35.0 (0.9)
ΔG_{bind}	**−9.5 (1.1)**	**−9.2 (0.9)**	**−15.5 (0.9)**	**−13.4 (1.0)**

[a] All values are in kJ mol^{-1}. Errors are given as standard error of the mean. Relevant data for 2-OG and 2-MPA are also reported for comparison.[12]

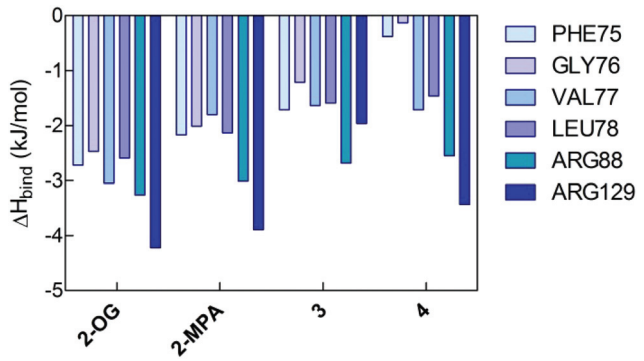

Fig. 4 Per-residue enthalpy contribution to the binding (ΔH_{bind}) of 2-OG, 2-MPA, **3** and **4** to NtcA. All values are in kJ mol^{-1}.

Gly76, Val77, and Leu78, drastically reduced to two stabilizing H-bond interactions in the case of **3** and **4**. The ultimate consequence is a considerably lower affinity of **3** and **4** for NtcA, as shown by the values listed in Table 1. Specifically, the NctA binding free energy (ΔG_{bind}) value of **3** is −9.5 kJ mol^{-1}, whilst that of **4** is −9.2 kJ mol^{-1}. With a corresponding decrement in ΔG_{bind} amounting to approximately to 6 kJ mol^{-1} compared with 2-OG, these two new derivatives are substantially weaker binders (Table 1).

To analyse in further detail the mode of binding of **3** and **4** to NtcA, the enthalpic term (ΔH_{bind}) of overall free energy of binding was deconvoluted into individual ligand–residue pairs to create the NtcA/residue interaction spectra shown in Fig. 4. These confirmed that the major stabilizing contributions in both complexes are indeed afforded by the salt bridges between the carboxylic acid moieties of the probes and the guanidinium groups of Arg88 and Arg129 in NtcA. They also clearly showed that these contributions are considerably less favourable in both **3** and **4**, than those observed for 2-OG and 2-MPA (Fig. 4 and Table 2). Further evidence of weak receptor binding by **3** and **4** is shown by the substantial reduction in the enthalpic stabilization offered by all other main NtcA residues involved in compound binding (*i.e.*, Phe75, Gly76, Val77, and Leu78) (Table 2 and Fig. 4). Altogether, our results confirm that the carbon skeleton of 2-OG with 5 carbon atoms is essential for its signalling function. Structural alteration with either longer or shorter skeleton length is not tolerated with regard to maintaining the signalling role of 2-OG.

Table 2 Per-residue enthalpy contribution to the binding (ΔH_{bind}) of 2-OG, 2-MPA, **3** and **4** to the NtcA[a]

	PHE75	GLY76	VAL77	LEU78	ARG88	ARG129
2-OG	−2.72	−2.47	−3.05	−2.59	−3.26	−4.22
2-MPA	−2.17	−2.01	−1.80	−2.13	−3.01	−3.89
3	−1.71	−1.21	−1.63	−1.59	−2.68	−1.96
4	−0.38	−0.13	−1.71	−1.46	−2.55	−3.43

[a] All values are in kJ mol^{-1}. Errors are in the range 0.01–0.03.

Conclusions

In this work, we conceived and synthesised the novel series of 2-OG probes **1**–**4** with the purpose of increasing our understanding of the structure–activity relationship of 2-OG analogues in mimicking the signalling role of 2-OG. Instead of the original two carboxylic groups in 2-OG, compounds **1** and **2** bear tetrazole and methyl ester functionalities, respectively. Thus, **1** and **2** are the probes of choice to examine the importance of the two carboxylic acid terminals in 2-OG in its signalling role. Compared with 2-OG, probes **3** and **4** feature a shorter and a longer molecular skeleton, respectively; accordingly, they were devised to assess the importance of the 2-OG carbon chain length in its signalling function. Among all these probes, **2** was endowed with substantial cellular toxicity for reasons yet unknown, while **1** could not be efficiently internalized by the cells. In contrast, compounds **3** and **4** were efficiently taken up by cells; however, they failed to promote DNA binding to the 2-OG receptor NtcA. Consequently, all these new probes failed to mimic 2-OG in triggering heterocyst formation in *Anabaena*. Notwithstanding these seemingly negative aspects, taken together these results yield important information on the structural requirements of 2-OG analogues to mimic the signalling role of 2-OG. Indeed, for the first time, this study unequivocally confirms that the two carboxylic acid terminals and the 5 carbon atom chain in 2-OG are both essential for the 2-OG signalling function, with even minor structural alteration or modification not being tolerated. Such insights into the structure–activity relationship of 2-OG mimics may be instrumental in conceiving effective, high affinity 2-OG probes with the ultimate goal of studying the complex yet intriguing signalling roles of 2-OG and its related signalling pathways.

Experimental section

General

All the reactions were carried out under argon. Compound **2** was synthesized according to the literature[11] and compound **3** was purchased from Sigma Aldrich. Anhydrous THF was distilled in the presence of sodium-benzophenone with a deep blue colour being persisted. All the other reagents were purchased from Sigma-Aldrich (China) or Acros Organics (China) without any further purification. Silica gel (200–300 mesh)

used for flash chromatography was purchased from Qing Dao Hai Yang Chemical Industry Co. in China. ^{1}H NMR and ^{13}C NMR spectra were recorded at 300 MHz and 75 MHz respectively on a Varian Mercury-VX300 spectrometer. ^{1}H HRMAS NMR spectra were recorded at 400 MHz on a Bruker Avance spectrometer. Chemical shifts are reported in parts per million (ppm). HRMS were determined by Waters Micromass GCT Premier.

Procedure for the preparation of 1

To a solution of 2-methyleneglutaronitrile (0.220 mL, 2.00 mmol) in toluene (12.0 mL) was added Et_3N·HCl (1.37 g, 10.0 mmol) and NaN_3 (650 mg, 10.0 mmol). The reaction mixture was refluxed for 9 h, and then was allowed to cool down to room temperature, followed by the addition of water (15.0 mL) and 1.0 M NaOH solution. The water phase was washed with ethyl acetate (3 × 15.0 mL), successively acidified to pH = 1–2 with 10% HCl and extracted with ethyl acetate (3 × 15.0 mL). The organic layers were combined, dried over $MgSO_4$, filtered and concentrated to give **1** as a pale yellow solid (288.6 mg, 75%). ^{1}H NMR (300 MHz, D_2O), δ 5.85 (s, 1H, C═CH*H*), 5.49 (s, 1H, C═CH*H*), 3.17 (t, J = 7.4 Hz, 2H, CH_2), 2.96 (t, J = 7.4 Hz, 2H, CH_2); ^{13}C NMR (75 MHz, D_2O), δ 153.5, 153.0, 127.6, 120.7, 28.4, 19.3; HRMS: calcd for $C_6H_8N_8$ 192.0872, Found 192.0874.

Procedure for the preparation of 4

To a suspension of NaH (60%, 240 mg, 6.00 mmol) in freshly distilled THF (5.00 mL) was added triethyl phosphonoacetate (1.21 mL, 6.00 mmol) in freshly distilled THF (5.00 mL) over a period of 30 min at 0 °C. The reaction mixture was stirred at room temperature for 30 min. After complete consumption of NaH, 4-bromobutyl acetate (0.730 g, 5.00 mmol) in freshly distilled THF (10.0 mL) was added into the reaction mixture over a period of 20 min at 0 °C. The solution was then refluxed for 3 h before quenching by the addition of a saturated NH_4Cl (10.0 mL), followed by extraction with ethyl acetate (3 × 10.0 mL). The combined organic layers were dried over anhydrous $MgSO_4$, filtered and concentrated under reduced pressure to obtain a crude residue. To the solution of this crude residue in THF (7.50 mL) was added 37% formaldehyde solution (5.00 mL, 60.0 mmol) and 25% K_2CO_3 solution (3.50 mL, 7.00 mmol). The reaction mixture was refluxed for another 3 h, and was then allowed to cool down to room temperature, followed by the addition of water (15.0 mL). The water phase was extracted with ethyl acetate (3 × 15.0 mL), the organic layers were combined, dried over $MgSO_4$, filtered and concentrated to obtain the crude residue. The crude residue was purified by flash chromatography using petroleum ether–ethyl acetate (8 : 1, v/v), yielding the diethyl ester intermediate as a colourless oil (891 mg).

To a solution of this diethyl ester precursor (423 mg, 2.00 mmol) in acetone (10.0 mL) at 0 °C was added 10.0 mL 2.5 M LiOH solution slowly. After stirring for 45 min at room temperature, the acetone was evaporated and the aqueous phase was washed with ethyl ether (3 × 15.0 mL). Then the aqueous phase was acidified to pH = 1–2 with 1.0 M HCl and extracted with ethyl acetate (3 × 15.0 mL). The organic layers were combined, dried over $MgSO_4$, filtered and concentrated to give **4** as a white solid (271 mg). The total yield of the two-step reaction is 71%. ^{1}H NMR: (300 MHz, D_2O), δ 6.01 (s, 1H, C═CH*H*), 5.54 (s, 1H, C═CH*H*), 2.22 (t, J = 7.2 Hz, 2H, $CH_2CH_2CH_2$), 2.16 (t, J = 7.2 Hz, 2H, $CH_2CH_2CH_2$), 1.60 (q, J = 7.2 Hz, 2H, $CH_2CH_2CH_2$); ^{13}C NMR: (75 MHz, DMSO-d_6), δ 174.91, 168.6, 141.1, 125.1, 33.6, 31.3, 23.9; HRMS: calcd for $C_7H_{10}O_4$ 158.0579, Found 158.0585.

Culture of the cyanobacterium *Anabaena* PCC 7120

The KGTP strain of *Anabaena* PCC 7120, expressing the 2-OG permease from *E. coli*, was constructed and cultured as described.[24] Cells were grown in BG11 medium in the presence of 5 mM ammonium as the nitrogen source. During the exponential phase of cell growth, $CuCl_2$ was added to a 0.8 M final concentration to induce the *kgtP* expression. After 18 h, 1 mM 2-OG analogue was added and heterocysts were observed under an optical microscope 24 h later.

HRMAS NMR

For HRMAS NMR measurement, cells from KGTP strain with O.D. = 0.4, grown under BG11 medium with ammonium, were incubated with 1 mM 2-OG analogues, collected at specific times by centrifugation and rinsed twice in BG11 with ammonium to remove the extracellular 2-OG analogues.

All HRMAS NMR spectra were recorded on a 400 MHz Bruker Avance spectrometer operating at a ^{1}H resonance frequency of 400.1 MHz. ^{1}H experiments were performed with a commercial 4 mm HRMAS ^{1}H–^{19}F/^{13}C probe head. About 2 mg of the cell sample was added to 50 μL of D_2O, to provide a deuterium lock, and sealed into a 4 mm zirconia rotor. To improve the resolution, samples were spun at a magic angle and the spinning rate was set at 4000 Hz. All experiments were recorded at room temperature.

^{1}H HRMAS NMR spectra were acquired using a CPMG spin-echo pulse sequence [90-(τ-180-τ)$_n$-acquisition] as a T_2 filter to remove the broad signals from large macromolecules. We used n = 150 to obtain a total spin–spin relaxation delay of $2n\tau$ = 75 ms. A 4.8 μs 90° pulse, with 1024 scans and a recycle time of 3 s were used. Chemical shift were referenced to TMS (at 0 ppm).

DNA binding activity of NtcA

A 170 bp DNA fragment corresponding to the *glnA* promoter region was amplified by PCR with the primers 5′ GGATTTTATGTCAAAGTTGACCCC 3′ and 5′ CGAAACAAAGTTGATGAC 3′. The NtcA protein was purified and the binding shift assay was performed as previously described using 0.18 μg DNA and 0.14 μg protein in 20 μL assay system.[32] The DNA bands were visualized after staining with ethidium bromide.

Computational details

The entire computational recipe involved the following program packages: *AutoDock* 4.2,[33] *Amber* 12,[34] *Discovery Studio*

(v.2.5, Accelrys Inc., San Diego, CA, USA), and in-house developed codes (stand-alone and add-on to the commercial software). The extensive, parallel molecular dynamics analyses were performed using running on the EURORA-GPU and FERMI supercomputers at the CINECA supercomputer center (Bologna, Italy).

The X-ray structures of NtcA in complex with 2-OG (PDB entry codes 3LA2.pdb)[34] were used as reference complexes. The model structures of the ligands were generated with *Discovery Studio*. All molecules were subjected to an initial energy minimization, with the convergence criterion set to 10^{-4} kcal (mol Å)$^{-1}$. A conformational search was carried out using a well-validated, *ad-hoc* developed combined molecular mechanics/molecular dynamics simulated annealing (MDSA) protocol, as previously described.[12,13]

The optimized structures of the test compounds were docked into the binding site of NtcA by applying a consolidated procedure.[12,13]

Each best substrate/NtcA complex resulting from the automated docking procedure was further refined in Amber 12 using the quenched molecular dynamics (QMD) method.[12,13,27,35] In this case, 1 ns molecular dynamics (MD) simulations at 310 K were employed to sample the conformational space of the ligand–NtcA complex in the GB/SA continuum solvation environment. The integration step was equal to 1 fs. After each ps, the system was cooled to 0 K, and the structure was extensively minimized, and stored. To prevent global conformational changes of the protein, the backbone of the protein binding site was constrained by a harmonic force constant of 100 kcal Å^{-1}, whereas the amino acid side chains and the ligands were allowed to move without any constraint.

The best energy configuration of each complex resulting from the previous step was allowed to relax in an 80 Å × 80 Å × 80 Å box of TIP3P water molecules.[36] The resulting system was minimized with a gradual decrease in the position restraints of the protein atoms. Finally, to achieve electroneutrality and to reach the physiological 150 mM ionic strength, a suitable number of Na^+ and Cl^- counterions were added to the system. Each hydrated complex system was gradually heated to 310 K in three intervals, allowing a 2 ns interval per 100 K, and then equilibrated for 5 ns at 310 K, followed by 20 ns of data collection runs, necessary for the estimation of the free energy of binding (*vide infra*). The MD simulations were performed at constant T = 310 K using the Berendsen *et al.* algorithm.[37] The particle mesh Ewald method was used to treat the long-range electrostatics. For the calculation of the binding free energy between NtcA and each compound in water, a total of 2000 snapshots were saved during the MD data collection period described above.

The binding free energy ΔG_{bind} of each protein/ligand complex in water was calculated according to the procedure termed Molecular Mechanic/Poisson–Boltzmann Surface Area (MM/PBSA), originally proposed by Srinivasan *et al.*[38] and described in detail in the original papers by Peter Kollman and his group.[39]

A *per residue* binding free energy decomposition was performed exploiting the MD trajectory of each given compound/NtcA complex, with the aim of identifying the key residues involved in the ligand–receptor interaction. This analysis was carried out using the MM/GBSA approach,[40,41] and was based on the same snapshots used in the binding free energy calculation.

The entire MM/PBSA computational procedure was optimized by integrating AMBER 12 in modeFRONTIER,[42] a multidisciplinary and multi-objective optimization and design environment.

Acknowledgements

We are grateful for the financial support from ANR PCV program ("ProKrebs" project), Région PACA, Wuhan University and Aix-Marseille Université. Yang Wang and Xinjun Liu are supported by overseas Ph.D. fellowships from China Scholarship Council. We also thank Ms Mei Cong for her help in studying the stability of the probes and Dr Emily Witty for English correction.

Notes and references

1 W. He, F. J.-P. Miao, D. C.-H. Lin, R. T. Schwandner, Z. Wang, J. Gao, J.-L. Chen, H. Tian and L. Ling, *Nature*, 2004, **429**, 188–193.
2 S. C. Hebert, *Nature*, 2004, **429**, 143–145.
3 S. Laurent, H. Chen, S. Bédu, F. Ziarelli, L. Peng and C.-C. Zhang, *Proc. Natl. Acad. Sci. U. S. A.*, 2005, **102**, 9907–9912.
4 A. B. F. Bourrellier, B. Valot, A. Guillot, F. Ambard-Bretteville, J. Vidal and M. Hodges, *Proc. Natl. Acad. Sci. U. S. A.*, 2010, **107**, 502–507.
5 S. Zhang and D. A. Bryant, *Science*, 2011, **334**, 1551–1553.
6 S. Gálvez, M. Lancien and M. Hodges, *Trend Plant Sci.*, 1999, **4**, 484–490.
7 M. Hodges, *J. Exp. Bot.*, 2002, **53**, 905–916.
8 A. Ninfa and P. Jiang, *Curr. Opin. Microbiol.*, 2005, **8**, 168–173.
9 C. Loenarz and C. J. Schofield, *Nat. Chem. Biol.*, 2008, **4**, 152–156.
10 R. A. Cairns and T. W. Mak, *Cancer Discov.*, 2013, **3**, 730–741.
11 H. Chen, S. Laurent, S. Bédu, F. Ziarelli, H.-L. Chen, Y. Cheng, C.-C. Zhang and L. Peng, *Chem. Biol.*, 2006, **13**, 849–856.
12 X. Liu, H. Chen, E. Laurini, Y. Wang, V. Dal Col, P. Posocco, F. Ziarelli, M. Fermeglia, C.-C. Zhang, S. Pricl and L. Peng, *Org. Lett.*, 2011, **13**, 2924–2927.
13 X. Liu, Y. Wang, E. Laurini, P. Posocco, H. Chen, F. Ziarelli, A. Janicki, F. Qu, M. Fermeglia, S. Pricl, C.-C. Zhang and L. Peng, *Org. Lett.*, 2013, **15**, 4662–4665.

14 M.-X. Zhao, Y.-L. Jiang, Y.-X. He, Y.-F. Chen, Y.-B. Teng, Y. Chen, C.-C. Zhang and C.-Z. Zhou, *Proc. Natl. Acad. Sci. U. S. A.*, 2010, **107**, 12487–12492.

15 L. V. Myznikov, A. Hrabalek and G. I. Koldobskii, *Chem. Heterocycl. Compd.*, 2007, **43**, 1–9.

16 B. S. Jursic and B. W. Leblanc, *J. Heterocycl. Chem.*, 1998, **35**, 405–408.

17 M. Wang, R. Zhu, Z. Fan, Y. Fu, L. Feng, J. Yao, A. Maggiani, Y. Xia, F. Qu and L. Peng, *Bioorg. Med. Chem. Lett.*, 2011, **21**, 354–357.

18 The formation of the tetrazole is safe and efficient under the catalysis of NEt_3·HCl in toluene.[19]

19 K. Koguro, T. Oga, S. Mitsui and R. Orita, *Synthesis*, 1998, 910–914.

20 W. S. Wadsworth and W. D. Emmons, *J. Am. Chem. Soc.*, 1961, **83**, 1733–1738.

21 J. C. Meeks and J. Elhai, *Microbiol. Mol. Biol. Rev.*, 2002, **66**, 94–121.

22 C.-C. Zhang, S. Laurent, S. Sakr, L. Peng and S. Bédu, *Mol. Microbiol.*, 2006, **59**, 367–375.

23 It might be possible that **2** could act as an active acceptor of Michael reaction to react with nucleophiles within biomolecules, hence leading to the immediate cell toxicity.

24 M. F. Vazquez-Bermudez, A. Herrero and E. Flores, *J. Bacteriol.*, 2000, **182**, 211–215.

25 J.-H. Li, S. Laurent, V. Konde, S. Bédu and C.-C. Zhang, *Microbiology*, 2003, **149**, 3257–3263.

26 J. Griffin, J. Pole, J. Nicholson and P. Carmichael, *Biochim. Biophys. Acta*, 2003, **1619**, 151–158.

27 F. Felluga, G. Pitacco, E. Valentin, A. Coslanich, M. Fermeglia, M. Ferrone and S. Pricl, *Tetrahedron: Asymmetry*, 2003, **14**, 3385–3399.

28 M. Mazzei, E. Nieddu, M. Miele, A. Balbi, M. Ferrone, M. Fermeglia, M. T. Mazzei, S. Pricl, P. La Colla and F. Marongiu, *Bioorg. Med. Chem.*, 2008, **16**, 2591–2605.

29 M. A. Pierotti, E. Tamborini, T. Negri, S. Pricl and S. Pilotti, *Nat. Rev. Clin. Oncol.*, 2011, **8**, 161–170.

30 C. Meyer, D. Schepmann, S. Yanagisawa, J. Yamaguchi, V. Dal Col, E. Laurini, K. Itami, S. Pricl and B. Wünsch, *J. Med. Chem.*, 2012, **55**, 8047–8065.

31 E. Laurini, P. Posocco, M. Fermeglia, D. L. Gibbons, A. Quintás-Cardama and S. Pricl, *Mol. Oncol.*, 2013, **7**, 968–975.

32 M. F. Vazquez-Bermudez, A. Herrero and E. Flores, *FEBS Lett.*, 2002, **512**, 71–74.

33 G. M. Morris, D. S. Goodsell, R. S. Halliday, R. Huey, W. E. Hart, R. K. Belew and A. J. klein, *J. Comput. Chem.*, 1998, **19**, 1639–1662.

34 D. A. Case, T. A. Darden and T. E. Cheatham, *et al.*, *AMBER 12*, University of California, San Francisco, CA, USA, 2012.

35 V. Frecer, M. Kabelac, P. De Nardi, S. Pricl and S. Miertus, *J. Mol. Graph. Model.*, 2004, **22**, 209–220.

36 W. L. Jorgensen, J. Chandrasekhar, J. D. Madura, R. W. Impey and M. L. Klein, *J. Chem. Phys.*, 1983, **79**, 926–935.

37 H. J. C. Berendsen, J. P. M. Postma, W. F. Van Gunsteren, A. DiNola and J. R. Haak, *J. Chem. Phys.*, 1984, **81**, 3684–3690.

38 J. Srinivasan, T. E. Cheatham III, P. Cieplak, P. A. Kollman and D. A. Case, *J. Am. Chem. Soc.*, 1998, **120**, 9401–9409.

39 P. A. Kollman, I. Massova, C. Reyes, B. Kuhn, S. Huo, L. Chong, M. Lee, T. Lee, Y. Duan, W. Wang, O. Donini, P. Cieplak, J. Srinivasan, D. A. Case and T. E. Cheatham III, *Acc. Chem. Res.*, 2000, **3**, 889–897.

40 A. Onufriev, D. Bashford and D. A. Case, *J. Phys. Chem. B*, 2000, **104**, 3712–3720.

41 M. Feig, A. Onufriev, M. S. Lee, W. lm, D. A. Case and C. L. Brooks III, *J. Comput. Chem.*, 2004, **25**, 265–284.

42 http://www.esteco.com/home/mode_frontier/mode_frontier.html.